Available online at www.sciencedirect.com
SCIENCE DIRECT
Vision Research 46 (2006) 2786–2797
Vision Research
www.elsevier.com/locate/visres

Imaging polarimetry of the circularly polarizing cuticle of scarab beetles (Coleoptera: Rutelidae, Cetoniidae)

Ramón Hegedüs [a], Győző Szél [b], Gábor Horváth [a,*]

[a] *Biooptics Laboratory, Department of Biological Physics, Physical Institute, Faculty of Natural Sciences, Eötvös University, H-1117 Budapest, Pázmány sétány 1, Hungary*

[b] *Coleoptera Collection, Department of Zoology, Hungarian Natural History Museum, H-1088 Budapest, Baross utca 3, Hungary*

Received 26 November 2005; received in revised form 30 January 2006

Abstract

The light reflected from the metallic-shiny regions of the cuticle of certain beetles belonging to the Scarabaeoidea is known since 1911 to be left-handed circularly polarized. Only photographs of a few selected species of scarabs, taken through left- and right-circular polarizers, have earlier been published. Through a right-circular polarizer these beetles appear more or less dark. This demonstration is, however, inadequate to quantitatively investigate the spatial distribution and the wavelength dependency of the circular polarization of light reflected from the scarab cuticle. In order to overcome this problem, we have developed a portable, rotating analyzer, linear/circular, digital, and imaging polarimeter. We describe here our polarimetric technique and present for the first time the linear and circular polarization patterns of the scarab species *Chrysophora chrysochlora*, *Plusiotis resplendens* (Rutelidae), and *Cetonischema jousselini* (Cetoniidae) in the red (650 nm), green (550 nm), and blue (450 nm) parts of the spectrum. We found the wavelength- and species-dependent circular polarization patterns in scarabs to be of a rather complex nature. These patterns are worthy of further studies.

Keywords: Scarab beetles; Scarabaeoidea; Coleoptera; *Chrysophora chrysochlora*; *Plusiotis resplendens*; *Cetonischema jousselini*; Metallic-shiny cuticle; Circular polarization; Ellipticity; Imaging polarimetry; Polarization pattern; Polarization vision

1. Introduction

Circularly polarized light is rare in nature. It occurs, for example when underwater linearly polarized light is totally reflected from the water–air interface outside the Snell window (Können, 1985, p. 149). The left and right lanterns of the firefly larvae *Photuris lucicrescens* and *Photuris versicolor* emit left- and right-handed circularly polarized light at a peak wavelength of 540 nm (Wynberg et al., 1980). The birefringent cuticle of certain crustaceans also reflects circularly polarized light (Neville & Luke, 1971), and the light passing through the semi-transparent body of certain dinoflagellates is also circularly polarized (Horváth & Varjú, 2003, pp. 100–103). According to Können (1985, p. 84), some tropical butterflies have a colored gloss caused by multiple reflections on the wingscales, and an accidental combination of reflections may convert unpolarized light into circularly polarized light in tiny spots on the wing depending on the angle of incidence.

The American physicist, Albert Abraham Michelson (1852–1931) discovered in 1911 that the light reflected from the scarab beetle *Plusiotis resplendens* had a left-handed circularly polarized component. Robinson (1966), investigating the chemical structure and optical properties of cholesteric liquid crystals and observing circularly polarized light reflected from them, became fascinated by the studies of Michelson (1911) and obtained a variety of beetles, with which he repeated Michelson's investigations. He found that the light reflected from these beetles was circularly polarized. He emphasized that "it would be of interest to consider what survival value can account for the occurrence of this most unusual property in so many species."

* Corresponding author.
E-mail address: gh@arago.elte.hu (G. Horváth).

0042-6989/$ - see front matter © 2006 Elsevier Ltd. All rights reserved.
doi:10.1016/j.visres.2006.02.007

The left-circular polarization of light reflected from the metallic-shiny regions of the cuticle of certain scarabs can be easily demonstrated by observing them through a right-circular polarizer, when the body appears more or less dark. The circularly polarized gloss spreads all over the body of some scarabs and is retained after the death of the animals. According to Können (1985, pp. 83–85) and Kattawar (1994), some mutant specimens may reflect not left-handed, but right-handed circularly polarized light. However, this phenomenon has never been documented in the literature.

The circular polarization of this metallic gloss is caused by the helical structure of the molecules of the chitinous cuticle (Caveney, 1971; Können, 1985, pp. 139–140; Neville & Caveney, 1969) . The direction of rotation of the electric field vector (*E*-vector) of circularly polarized reflected light depends on the sense of rotation of the helix of the molecules. In living organisms, the capability to produce a given helical molecule is restricted to one sense of rotation, which has been fixed at a very early stage in evolution. Thus, perhaps apart from some mutants, this sense is the same for all living organisms. Since the exoskeletons of all beetles reflecting circularly polarized light consist of the same substance, the sense of rotation of the *E*-vector of reflected light is the same, left-handed, for all of them (Können, 1985, pp. 83–85).

The observation that circularly polarized light is reflected from the cuticle of certain scarabs raises the question whether the eyes of these beetles are able to perceive circular polarization. The answer is unfortunately unknown. As far as we know (Horváth & Varjú, 2003), the photoreceptors investigated until now cannot discriminate between left- and right-handed circularly polarized light, and they could not discriminate between elliptically and partially linearly polarized light with the same degrees and angles of polarization.

In the literature, only sporadic photographs taken from a few scarab species (e.g., *P. resplendens*, *Plusiotis woodi*, and *Cetonia aurata*) through left- and right-circular polarizers are available (e.g., Kattawar, 1994; Können, 1985, p. 83). This demonstration is, however, inadequate to quantitatively investigate the spatial distribution and the wavelength dependency of the circular polarization of light reflected from the metallic-shiny cuticle of scarabs. To our knowledge, quantitative measurements of the circular polarization patterns of scarab beetles have not been published so far. This motivated us to measure both the linear and circular polarization patterns of scarabs in the red, green, and blue parts of the spectrum. In order to accomplish this, we have developed a portable, rotating-analyzer, linear/circular, digital, and imaging polarimeter. We found the wavelength- and species-dependent circular polarization patterns to be of a rather complex nature, which are worthy of further studies. In this paper we describe the theoretical and experimental background of our imaging polarimetric method, and present for the first time the linear and circular polarization patterns of the metallic-shiny cuticle of three scarab species.

2. Materials and methods

Our portable, rotating-analyzer, linear/circular, and imaging polarimeter consists of a Nikon Coolpix 4500 digital camera, one right-handed and three left-handed B+W KSM 28 C-POL MRC circular polarizers with 28 mm diameter (Fig. 1A). The polarizers are placed on a metal filter wheel (Figs. 1B and C). The filter wheel can be manually rotated between discrete directions, thus any of the four polarizers can be set in front of the objective lens of the camera. The first three polarizers (filters 1, 2, and 3) mounted normally in front of the camera function as linear analyzers, in which the angle of the transmission axis is 90°, 150°, and 30° relative to the radius of the filter wheel (Fig. 1B). Thus the angles characterizing these left-circular polarizers (linear analyzers) as defined in the Appendix A are $\theta_1 = 135°$, $\theta_2 = 15°$, and $\theta_3 = 75°$ (Fig. 7). The fourth polarizer (filter 4) that is mounted reversed, functions as a circular analyzer (Fig. 1B)[1]. Fig. 1C shows the arrangement of the filters in front of the camera from the side.

To illuminate the target (insect to be investigated) uniformly from the left, right, top, and bottom, we use a rotationally symmetric illumination called ''omnidirectional'' further on in this work. Omnidirectional illumination is performed by two concentric, circular light tubes (Fig. 1D) emitting continuously white, UV-deficient light. The height of the two light tubes can be adjusted between 7 and 15 cm from the base, and can be switched on/off separately. The target is placed along the axis of rotation of the circular tubes at the centre of the base of the lamp. During the measurement the polarimeter is fixed on a tripod and the omnidirectionally illuminated target is photographed through all four polarizers (Figs. 1E and F). The measurement begins only 10–15 min after switching on the light source, when the spectrum of the emitted light is already constant. (The spectrum of the light tubes changes significantly during the gradual warming-up of the tubes.) The light tubes are covered by an annular card screening the camera that focuses to the illuminated target. All automatic image manipulation functions of the digital camera (e.g., smoothing, noise reduction, and contrast enhancement) are switched off, and the focus, aperture, time of exposure are set manually, so that all four polarizational pictures at a given target are taken with the same settings. Using a piece of blank white paper at the place of the target, the camera is ''white balanced'' prior to the first measurement. To eliminate any displacement of the camera, the expositions are performed by a Nikon MC-EU1 remote cord.

The preview picture of the target is transmitted from the camera's video output to the 15″ monitor of a Sony Vaio PCG-9S1M portable (laptop) computer by a Terratec Cinergy 200 TV tuner connected to the USB port of the computer. The magnified preview picture visible on the monitor enables an appropriate manual control of the focus and other optical parameters. The four polarizational digital pictures of a given target are transmitted to the laptop computer through its USB port. These pictures are stored in uncompressed, true color TIFF format and are evaluated by a computer program written by us. The evaluation is based on the formulae Eq. (17) giving the components S_0, S_1, S_2, and S_3 of the Stokes vector $\underline{S}$ of the light reflected from the target towards the polarimeter (see Appendix A). The intensity $I = S_0$, degree of linear polarization p, angle of polarization α (measured from the reference y–z plane in Fig. 1F) and ellipticity ε described by Eq. (18)–(20) are then calculated from the Stokes vector $\underline{S}$ and visualized with color coding. The resolution of the pictures taken by the Nikon Coolpix 4500 digital camera is 4 Megapixels with 8 bit color

[1] Note that in this paper we consistently use the formalism and nomenclature of Collett (1993), regarding polarization and polarization filters. In this nomenclature these filters are named according to their active-side function (that means: how they transform incoming light), that is: ''left-/right-circular polarizer'' and ''reversed left-/right-circular polarizer'', while according to their passive-side function (that means: what can we analyze by measuring the intensity of light passing through them) they can be termed as ''linear analyzer'' and ''left-/right-circular analyzer,'' respectively. We apply both terms where explicitly necessary. See Appendix A for further details.

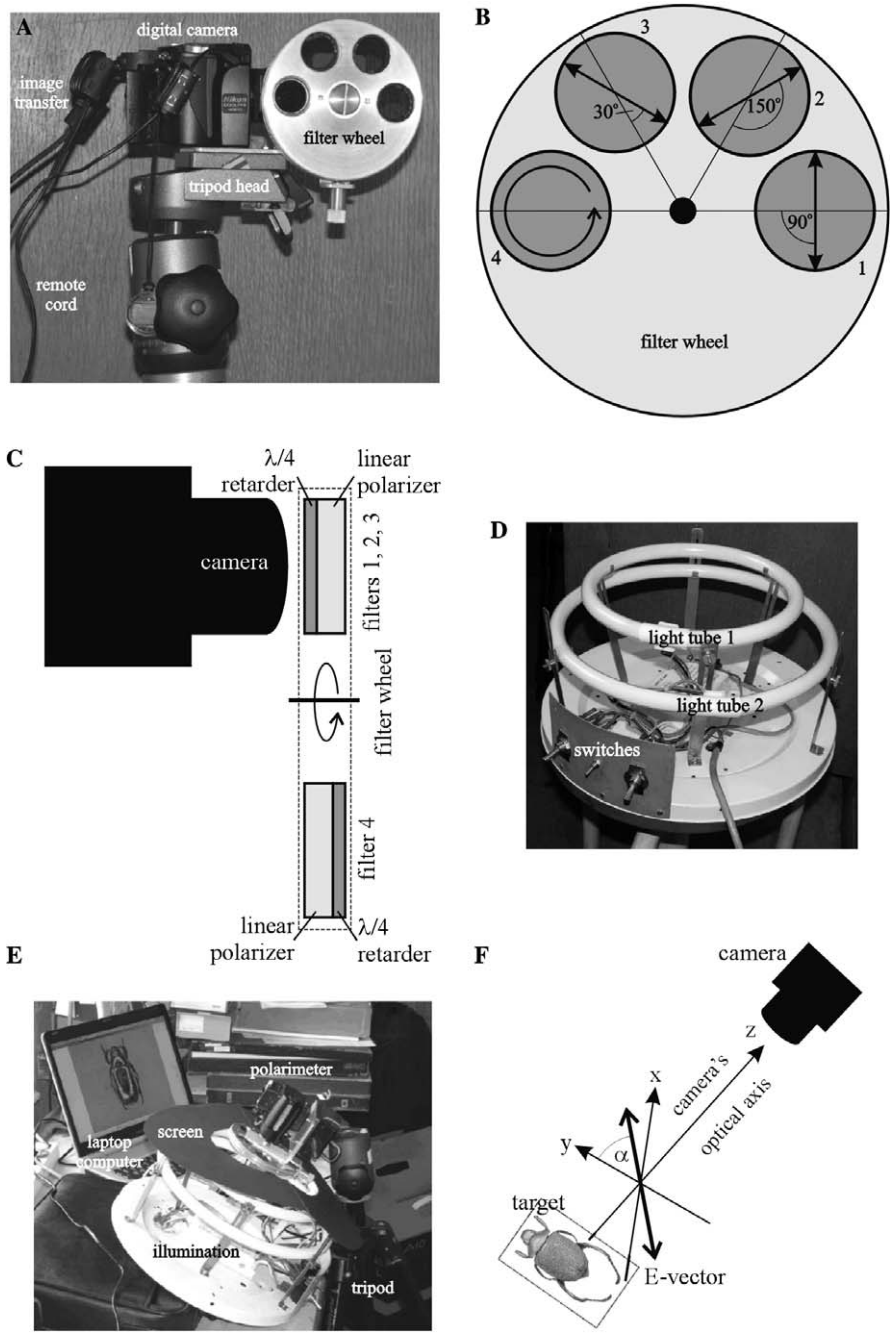

Fig. 1. (A) Photograph of our portable, rotating-analyzer, linear/circular, and imaging polarimeter. (B) Filter wheel of the polarimeter with the four polarizers as seen by the camera. Filters 1–3 are left-handed circular polarizers, while filter 4 is a reversely mounted right-handed circular polarizer. Filters 1–3 function as linear analyzers, the transmission axes of which are represented by double-headed arrows. Angles 90°, 150°, and 30° are measured from the radius of the filter wheel. Filter 4 functions as a circular analyzer, in which the transmission axis of the linear polarizer component is arbitrarily aligned (and therefore is not displayed). The circular arrow represents the handedness of the circular polarizer 4. (C) Arrangement of the filters in front of the camera from the side. (D) Annular light source composed of two concentric, circular light tubes illuminating the target (scarab beetle) positioned along the axis of rotation of the tubes. These tubes produce a rotationally symmetric "omnidirectional" illumination. (E) Setup of the measurement. (F) Reference system of coordinates for the description of light polarization. The x–y plane corresponds to the plane of the piece of paper. The angle of polarization α (that is the alignment of the E-vector of linearly polarized light) is measured from the y–z plane, which is the plane of reference of the Stokes vector.

resolution for each color (red, 650 nm; green, 550 nm; and blue, 450 nm) channel. Since at every pixel the intensity measurement is carried out in the red, green, and blue channels, finally, we obtain the polarization patterns of the target separately in these three parts of the spectrum. The evaluation and visualization of the four polarizational pictures of a given target takes 1.5–2 min, which enables us to check in situ the quality of the pictures and patterns, the appropriateness of the illumination, and the settings of the camera's optical parameters. If any of these parameters is not appropriately set, the measurement is repeated with another, more adequate parameter configuration.

Our measurements have been carried out on air-dried specimens from the Coleoptera Collection of the Hungarian Museum of Natural History in Budapest. During the measurements the following phenomena can cause errors, and should, therefore, be eliminated, avoided, or minimized:

- *Inhomogeneous parameter setup.* Occurs if the four polarizational pictures of a given target are taken under different illumination conditions and/or with different settings of the optical parameters of the camera. This source of error has always been entirely eliminated.
- *Targetal motion artefact.* Originates from the displacement of the target relative to the camera during the exposition of the four polarizational pictures. Such artefacts are especially striking at the target's edges. This type of error has also been always eliminated by (i) careful manual rotation of the filter wheel, (ii) firm fixing of the target, and (iii) the use of an electronic remote cord for the exposure.
- *Environmental reflection-motion artefact.* The metallic-shiny cuticle of certain Scarabaeoidea species (e.g., *P. resplendens* that has been examined by Michelson in 1911) resembles a convex mirror, in which the surrounding objects (e.g., the filter wheel and the operator of the polarimeter) are inevitably mirrored. If any part of these mirror images changes during taking the four polarizational pictures of the target, motion artefacts appear after evaluation. This error cannot be fully eliminated, but it can be reduced by minimizing the motion of the surrounding objects and the operator during measurements. However, the rotation of the mirror image of the filter wheel is unavoidable, thus resulting in inevitable motion artefacts.
- *Mirror image of the illuminating light source.* If the surface of the investigated insect is smooth and shiny, the mirror images of the circular light tubes unavoidably appear on the cuticle. In these regions the pictures become overexposed, thereby falsifying the measured data. This kind of disturbance has been reduced by illuminating smooth and shiny insects by only one of the two light tubes, or by the ambient (sun and/or sky) light.
- *Inaccurate alignment of the polarizers.* The directions θ_1, θ_2, and θ_3 (see Appendix A) of the optical axes of the $\lambda/4$ retarders in the circular polarizers were set with an inaccuracy of $\pm 1°$. A more accurate alignment would not have made sense, because the quantum noise, described in the next point, can cause much greater errors.
- *Underexposition and quantum noise.* Underexposition has the consequence that the relationship between the measured intensities (belonging to the four polarizational pictures) and the Stokes vector (S_0, S_1, S_2, and S_3) becomes non-linear (see Appendix A). On the other hand, the errors of the degree of linear polarization p, angle of polarization α and ellipticity ε originating from the quantum noise of the digital pictures rapidly increases as the intensity $I = S_0$ decreases, because these errors are inversely proportional to S_0. Therefore, during the measurements it is best to avoid situations close to underexposition. Furthermore, for small values of S_3 (i.e., when the light to be measured is weakly circularly polarized) the error $\Delta_q\varepsilon$ defined in the Appendix A becomes significant. Since the pictures taken by the Nikon Coolpix 4500 digital camera have 8 bit color resolution per color (red, green, and blue) channel, the quantum noise of the measured intensity in one color channel is $\Delta q = \pm 1/255$. During the evaluation, by substituting $\Delta q = \pm 1/255$ into Eq. (22), we calculated the relative error $\Delta_q\varepsilon/\varepsilon$ of the ellipticity ε, which can reach 100% in those parts of a picture, where the intensity I and/or the ellipticity ε is very small. Therefore, during the evaluation we considered the pixels circularly unpolarized at which $|\varepsilon| < 4°$, because in this case the relative error $\Delta_q\varepsilon/\varepsilon$ was around 100%. Furthermore, pixels with relative error $\Delta_q\varepsilon/\varepsilon > 10\%$ were considered unevaluable. There are two possibilities to reduce the errors originating from the quantum noise: (i) using a digital camera with a greater (10–14 bit instead of 8 bit for each color channel) dynamical range. Unfortunately, such a digital camera was not available for us. (ii) Grouping a certain number of neighboring pixels and considering them as one pixel by summing up their intensity values. We considered 4 adjacent pixels as one pixel during the evaluation. This means that the new pixels have practically 10 bit resolution per color channel. Thus the quantum noise of intensity values in these new pixels ($\Delta q = \pm 1/1020$) is one fourth of that in the original pixels ($\Delta q = \pm 1/255$). The disadvantage of this process is that also the resolution of the final picture is reduced to one fourth (1 Megapixel) of that of the original one (4 Megapixel). The results shown in Figs.2–6 were obtained by this method of grouping.

3. Results

About 20% of the species in both Rutelidae and Cetoniidae families have entirely or partially metallic-shiny body. Beetles with circularly polarizing cuticles occur among these metallic insects. However, we experienced that not all metallic body parts reflect circularly polarized light. Here, we present the linear and circular polarization patterns of three species, the names, family names, and body sizes of which are listed in Table 1. Figs. 2–6A–C show the three investigated scarab beetles seen under three conditions: (A) through a reversed left-circular polarizer (left-circular analyzer), (B) with the naked eye, and (C) through a reversed right-circular polarizer (right-circular analyzer). Beetles strongly polarizing the reflected light left-circularly become darker and brighter relative to the background when seen through a reversed right- and left-circular polarizer, respectively (Figs. 2–6). The intensities of light passing through a reversed left-circular polarizer (rev LCP) and a reversed right-circular polarizer (rev RCP) are $I_{\mathrm{revLCP}} = (S_0 - S_3)/2$ and $I_{\mathrm{revRCP}} = (S_0 + S_3)/2$, where S_0 and S_3 are the components of the Stokes vector of the light passing through the polarizer (see Appendix A). Consequently, those parts of the cuticle brighten through a revLCP which darken through a revRCP, and vice versa. This brightening and darkening effect depends on the degree and handedness of the circular polarization characterized by S_3 (for left-circular polarization $S_3 < 0$, and for right-circular polarization $S_3 > 0$).

Since the linear polarization of light reflected from beetles could have already been measured earlier with imaging polarimetry (Horváth & Varjú, 2003), and because in the present paper, we focus on the circular polarization patterns, among the patterns in Figs. 2–6 we analyze in detail only those, which are related to circular polarization, that is the ellipticity patterns. For the sake of completeness, however, we also plotted the patterns related to linear polarization (i.e., degree of linear polarization p and angle of polarization α) in the red (650 nm), green (550 nm), and blue (450 nm) parts of the spectrum.

Figs. 2 and 3 show the reflection–polarization patterns of *Chrysophora chrysochlora* from above and the side. The dorsal surface of this beetle is rough, matt. In the patterns of ellipticity (Figs. 2M–O) we can see that in the green the entire dorsal side, the head and the legs (except for the last segments) reflect left-circularly polarized light, in the red some dorsal patches reflect circularly unpolarized, or left-, or right-circularly polarized light, while in the blue the head and the dorsal side is predominantly right-circularly polarizing, and some parts of the legs are also left-, or right-circularly polarizing. Interestingly, the last, bluish segments of the posterior legs reflect circularly unpolarized light in the red and green, but left-circularly polarized light in the blue. The finding that in the green the entire dorsal surface of the beetle is strongly left-circularly polarizing is already apparent if the beetle is seen through a right-circular polarizer (Figs. 2B and C). The dorsal side

Table 1
The scientific name, english names, family name, and body size of the scarab species studied

Scientific name	English vernacular names	Family name	Body size
Chrysophora chrysochlora (Latreille, 1812)	Longleg scarab beetle, green ruteline	Rutelidae	25–30 mm
Plusiotis resplendens (Boucomont, 1878)	Golden scarab beetle, gold beetle	Rutelidae	25–30 mm
Cetonischema jousselini (Gory & Percheron, 1833)	Flower chafer	Cetoniidae	20–30 mm

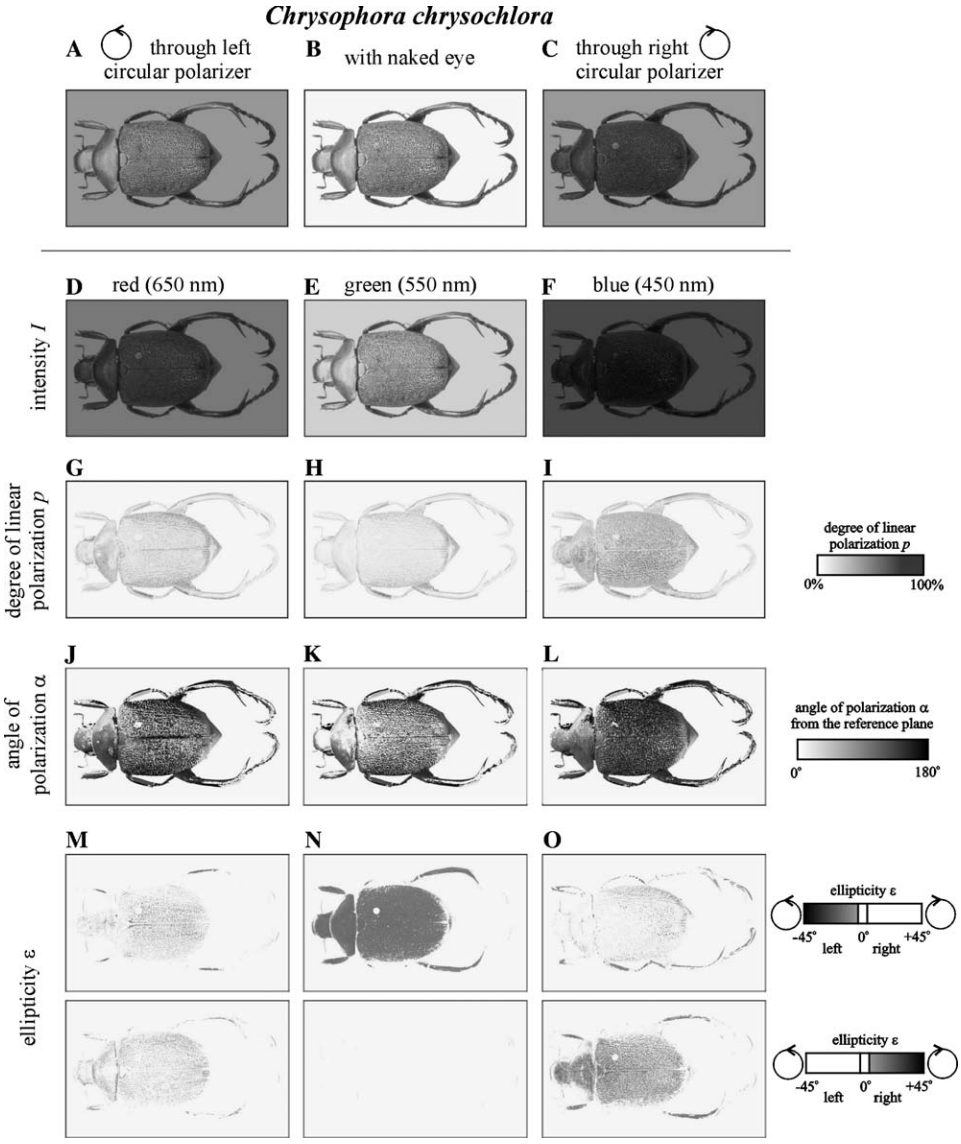

Fig. 2. Linear and circular polarization patterns of the scarab beetle *C. chrysochlora* measured by imaging polarimetry in the red (650 nm), green (550 nm), and blue (450 nm) ranges of the spectrum. The upper row shows the appearance through a reversed left-circular polarizer (A), a reversed right-circular polarizer (C) and without filter (B). Below A–C, the panels are sorted by wavelength (650, 550, and 450 nm). Rows D–F, G–I, J–L, and M–O display the intensity I, degree of linear polarization p, angle of polarization α (measured from the y–z reference plane in Fig. 1F) and ellipticity ε. The illumination of the beetle was omnidirectional due to the two circular light tubes. (For interpretation of the references to color in this figure legend, the reader is referred to the web version of this paper.)

of *C. chrysochlora* has a bluish-reddish patchy pattern. Both the dorsal and ventral surfaces of *C. chrysochlora* are similarly strongly circularly polarizing (Fig. 3): in the green the entire ventral side is left-circularly polarizing, in the red the reflected light (apart from some smaller patches) is mostly circularly unpolarized, while in the blue certain ventral patches are left-, or right-circularly polarizing. In Fig. 3 we can again see that the light reflected from the last segments of the legs is left-circularly polarized in the blue, but unpolarized in the red and green.

Figs. 4 and 5 show the reflection–polarization patterns of *Cetonischema jousselini* from above and the side. The head and the elytra of this beetle are metallic-green, while the thorax and the triangular shield are metallic-red. In

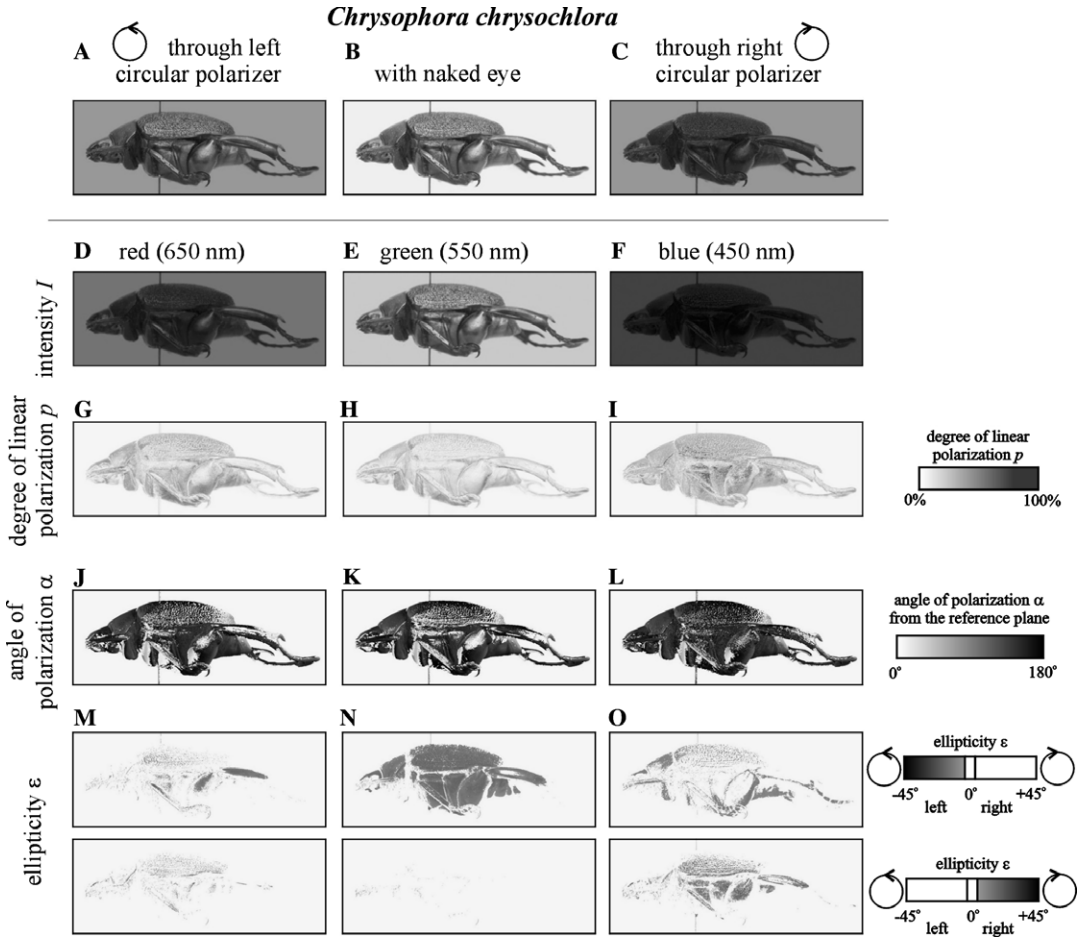

Fig. 3. As Fig. 2 from the side.

the green spectral range the green head and elytra reflect strongly left-circularly polarized light, but in other spectral ranges they are only weakly circularly polarizing (Figs. 4M–O). Both the red thorax and red shield are strongly left-circularly polarizing in the red, while weakly right-circularly polarizing in the green and blue (Figs. 4M–O). This explains why the beetle appears completely black when seen through a right-circular polarizer (Fig. 4C): then both the left-circularly polarized green light reflected from the head and elytra, and the left-circularly polarized red light reflected from the thorax and shield are filtered out. In Fig. 5 we can see that both in the green and red spectral ranges the entire ventral side, while in the blue only some ventral areas of *C. jousselini* are strongly left-circularly polarizing. There is no significant contrast in circular polarization between the dorsal and ventral sides of the beetle.

Since Michelson (1911) discovered the circular polarization of reflected light while studying the striking metallic gloss of the scarab beetle *P. resplendens*, it seems appropriate to present and analyze also the reflection–polarization patterns of this species (Fig. 6). The dorsal part of *P. resplendens* has a very strongly reflecting, metallic-shiny cuticle sparkling in yellowish-green. At first glance we could expect that *P. resplendens* is strongly circularly polarizing. However, the light reflected from the dorsal surface of *P. repslendens* is practically circularly unpolarized in the red and green ranges of the spectrum, and it is only weakly left- or right-circularly polarized in the blue in some tiny spots. Seen from above (not shown here), only the legs polarize light strongly left-circularly. In the red and green the entire ventral side, while in the blue only some ventral areas of *P. resplendens* are strongly left-circularly polarizing (Figs. 6M–O). Hence, there is a great ellipticity contrast between the dorsal (weakly circularly polarizing) and ventral (strongly circularly polarizing) half of the beetle. Based on these findings, we conclude that Michelson (1911) might have discovered the circular polarization of cuticle-reflected light by investigating the ventral surface and/or the legs of *P. resplendens* rather than studying the sparkling dorsal part, since the latter reflects practically circularly unpolarized light.

Finally, the linear polarization patterns are briefly analyzed here only for *C. chrysochlora* seen from above (Fig. 2). Similar results were obtained for *C. jousselini* (Figs. 4 and 5). Since the cuticle of *C. chrysochlora* is green (Fig. 2B), the intensity of light reflected from its surface is high in the green (Fig. 2E), but low in the red and blue

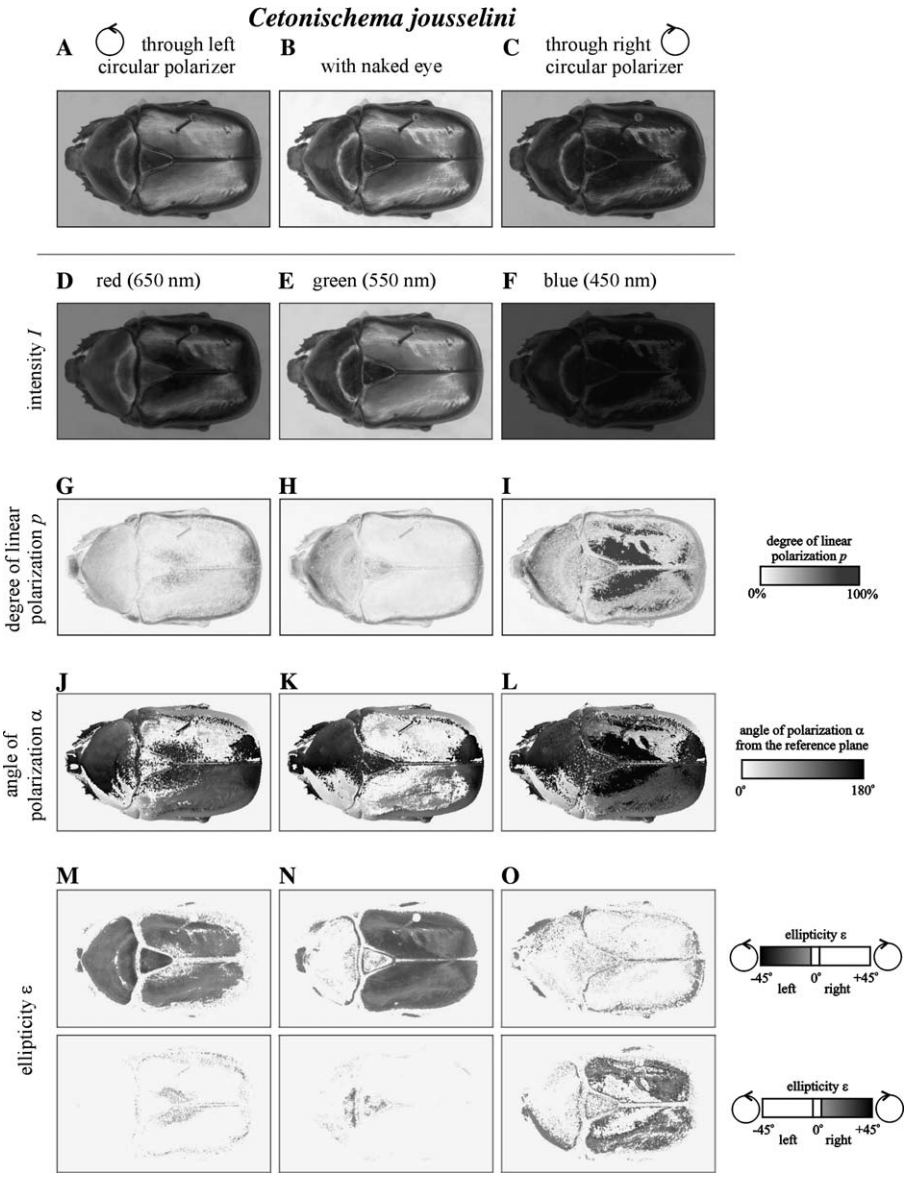

Fig. 4. As Fig. 2 for *C. jousselini*.

(Figs. 2D and F). The degree of linear polarization p of reflected light was quite low in all three spectral ranges (Figs. 2G–I), because the cuticle surface was more or less perpendicular to the optical axis of the polarimeter, and according to the Fresnel formulae, p of reflected light is very low at reflection angles ≈90° from the surface. Only, the downward-bending margin of the body make an exception, from where the light is reflected at an angle close to the Brewster's angle: here p is maximal. The p of the light reflected from the green cuticle is lowest in the green spectral range (Figs. 2G–I), which is due to the Umow effect (Umow, 1905). The angle of polarization α of light reflected from the convex cuticle is always 90° relative to the plane of reflection. Since the beetle was omnidirectionally illuminated, the angle of polarization α of light reflected from the elytra is ≈90°, while that reflected from the head, thorax and abdomen tip is nearly 0° (Figs. 2J–L). The α-pattern of the cuticle depends only slightly on the wavelength, i.e., it is nearly the same in the red, green, and blue spectral ranges.

4. Discussion

As circularly polarized light is rare in nature, and it is unknown whether any organism is able to perceive circular polarization (Horváth & Varjú, 2003), few efforts have been made to measure it. Our study tries to fill partially this gap. We developed a portable digital imaging polarimeter by which besides the patterns of linear polarization also the pattern of the circular polarization (i.e., ellipticity) of reflected light can be measured in the red, green, and blue parts of the spectrum. For the first time we present here the linear and circular polarization patterns of the metallic-shiny *C. chrysochlora*, *C. jousselini*, and *P. resplendens*.

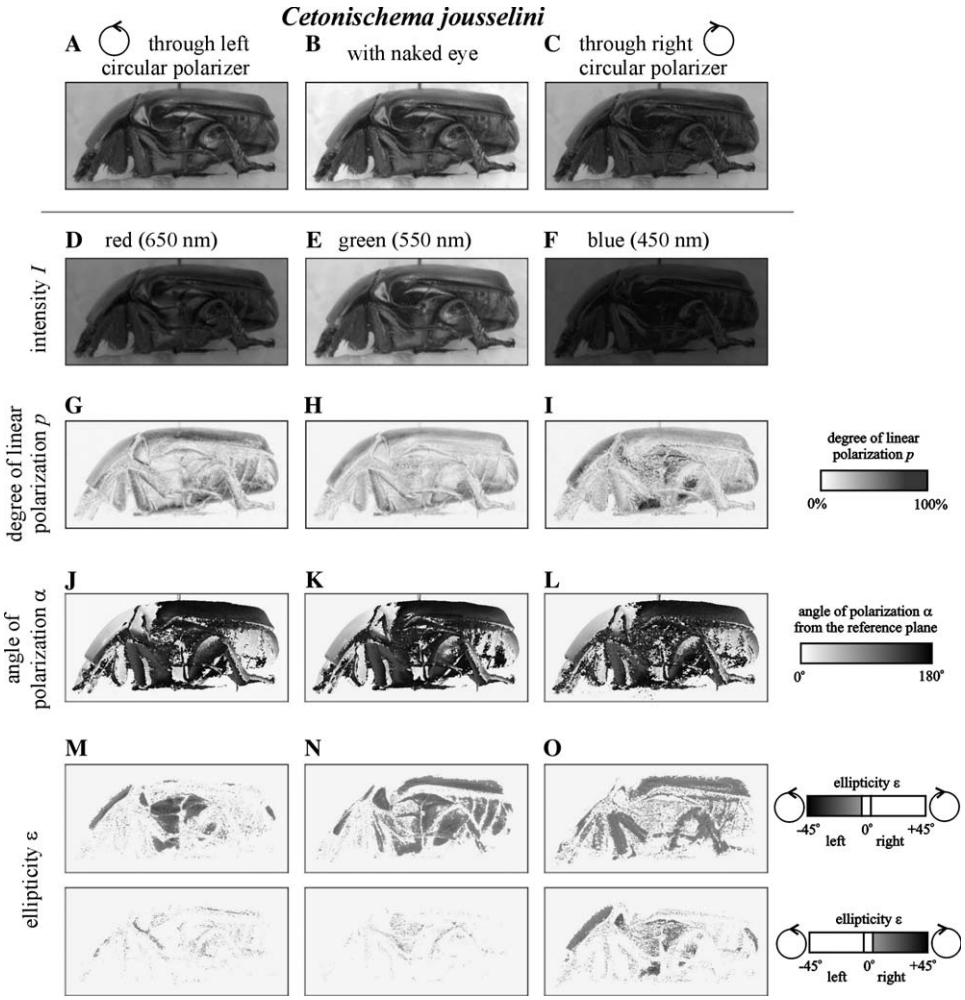

Fig. 5. As Fig. 4 from the side.

We selected these species for the following reasons: (i) they belong to two different scarab families (Rutelidae and Cetoniidae), (ii) *C. chrysochlora* and *C. jousselini* have strongly circularly polarizing cuticles, (iii) *C. chrysochlora* displays a relatively homogeneous green metallic color, while the cuticle of *C. jousselini* is red-, green-, and blue-colored, thus their circular polarization patterns are strongly wavelength dependent, and (iv) *P. resplendens* is historically important due to the discovery by Michelson (1911).

Albeit the circular polarization of light reflected from certain scarabs has been discovered by Michelson in 1911, to our knowledge until now no measurements of the spatial distribution of both linear and circular polarization of light reflected from insects have been carried out yet. On the basis of our results we conclude that it is worth investigating metallic-shiny scarab beetles by circular imaging polarimetry, since our measurements provide much more quantitative information about the circular polarization patterns (Figs. 2–6M–O) than simple, demonstrative photographs taken through circular polarizers (Figs. 2–6A and C). Using our new method, we experienced that there are species- and wavelength-dependent circular polarization patterns of metallic-shiny scarabs, and the phenomenon is much more complex than it has been thought earlier. The patterns in Figs. 2–6 characterize all polarizational information of light reflected from the cuticle of the investigated scarabs available in the red, green, and blue parts of the spectrum.

Compared to the presentation of the photographs taken through left- and right-circular polarizers, our new imaging polarimetric measurements add the significantly new aspect that the wavelength dependency of the circular polarization pattern can be quantitatively determined. From the photo pair it could be established neither quantitatively, nor qualitatively how the circular polarization varies in different spectral ranges. The following examples from among our results demonstrate well such variations, which would otherwise remain hidden when only seeing simple photographs:

- The right-circular polarization of light reflected from the cuticle of *C. chrysochlora* in the blue (Fig. 2O).
- The strong left-circular polarizing capability of the green cuticle of *C. jousselini* in the red spectral range (Fig. 4M), the nearly zero circular polarizing capability

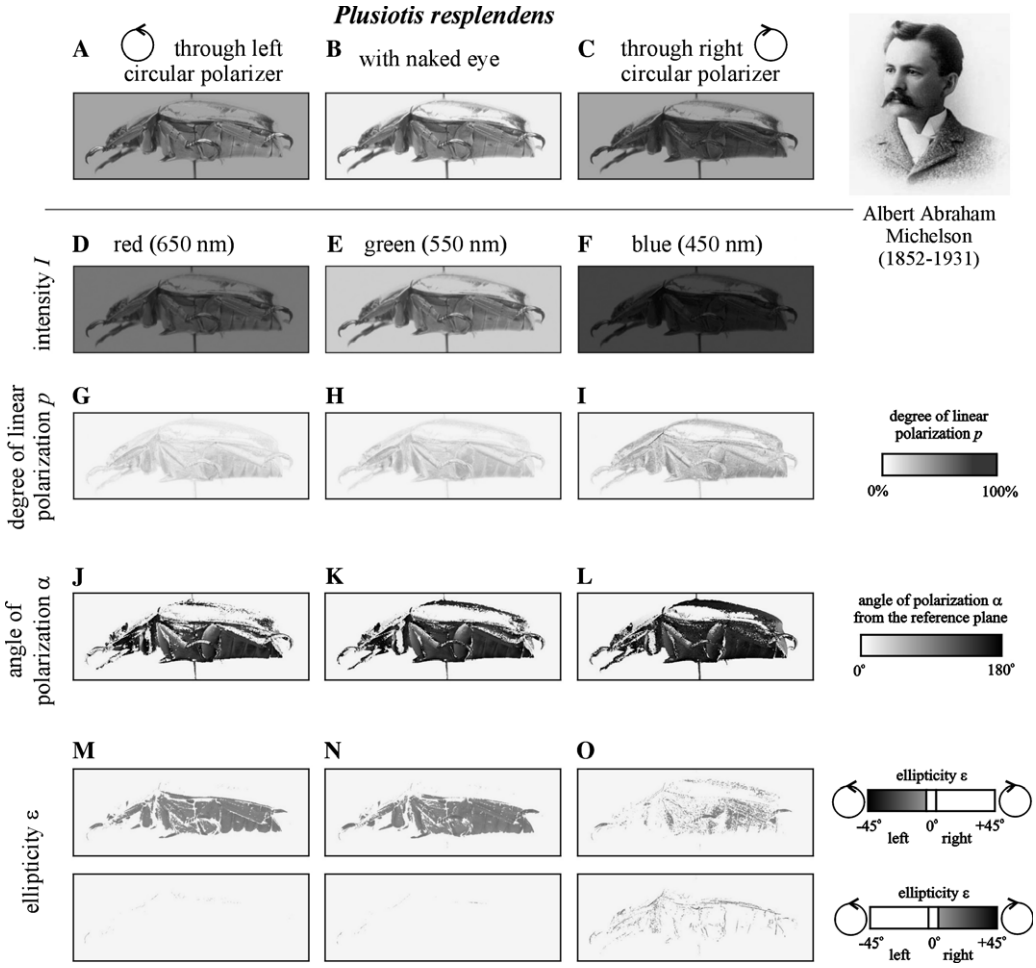

Fig. 6. As Fig. 3 for *P. resplendens*. The beetle was illuminated by diffuse ambient light (in order to avoid the disturbing mirror image of the two circular light tubes; Fig. 1C). The inset in the top right corner shows the portrait of the Nobel laureate American physicist, Albert Abraham Michelson (1852–1931), who discovered in 1911 that the light reflected from the cuticle of *P. resplendens* is left-circularly polarized.

of the red cuticle in the green spectral range (Fig. 4N), furthermore the right-circular polarizing capability of the green cuticle and the very low circular polarizing capability of the red cuticle in the blue spectral range (Fig. 4O).

- The complicated wavelength-dependence of the circular polarization pattern of light reflected by the red, green and blue cuticle parts of *C. jousselini* seen from the side (Figs. 5B and M–O).

Our circular polarimetric investigations may inspire biologists to find out whether the metallic-shiny, circularly polarizing scarab beetles can perceive circular polarization, and if so, whether they are able to distinguish between linear and circular polarization. The anatomical prerequisite for such perception could be a ''filter'' in front of microvillous photoreceptors being sensitive to linear polarization. Then, the filter and the microvilli of the receptors could function as a $\lambda/4$ retarder and a linear polarizer, respectively, and thus the whole system could operate as a circular polarizer. Although until now nobody has published any data about such a retarder in insect eyes, it is also unknown if such a structure has been sought for at all in animal eyes (Horváth & Varjú, 2003). Although the ultrastructure of the eyes of numerous ruteline and cetonid beetles, some related to the ones investigated in this work, were studied by Gokan and Meyer-Rochow (2000), it is unknown whether these insects are or are not sensitive to circular polarization.

The scarab species studied in this work belong to two families of Scarabaeoidea: Rutelidae and Cetoniidae. The family Rutelidae comprises ≈200 genera and 4100 species distributed worldwide. Rutelidae are generally called leaf chafers, the most colorful species often jewel scarab beetles. Ruteline beetles have diverse shapes and colors—some are metallic silver and gold, e.g., the *Plusiotis* species at which Michelson (1911) discovered the circular polarization of reflected light. Adult rutelines are phytophagous and feed on leaves or flowers of trees and shrubs. Adult leaf chafers emerge with a soft and pale cuticle, but within hours, their bodies harden and the jewel scarabs show their true, often splendid and metallic-shiny colors. The family Cetoniidae, comprising more than 400 genera and 3200 species distributed worldwide, is a group of beetles commonly known as

flower beetles (or fruit chafers, or flower chafers). They are diurnal and mostly colorful species of various sizes. Some of them are metallic green, red, blue, or purple, with the majority of the iridescent species occurring in the tropics. The members of this group are mostly pollen-feeders and are usually found on flowers. On the other hand, adults of the flower chafers prefer to eat nectar, sap and the juice and flesh of soft, ripe fruits. Their main predators are carnivorous birds and mammals. It would be an interesting task to study the possible circular polarization patterns in the optical environment of these beetles: as far as we know, the circular polarizing capability of leaves, fruits and flowers eaten by leaf, fruit, and flower chafers have not been investigated.

Acknowledgments

Many thanks for the financial support of the Hungarian Ministry of Education. This paper is based on the competition essay awarded by the 2005 Youth Bolyai Prize, the theme of which was determined by Prof. Zsolt Bor (Dept. of Optics and Quantum Electronics, Univ. Szeged, Hungary), the winner of the 2004 Bolyai Prize. We are grateful to Sándor Hopp (Mechanical Workshop, Physical Inst., Eötvös Univ., Budapest) for constructing the mechanical components of our polarimeter. We also acknowledge the help of László Fogl (Dept. Biological Physics, Eötvös Univ.) for constructing the light source of our polarimeter. We thank Dr. Ottó Merkl (head of the Coleoptera Collection) for enabling us the polarimetry on scarabs in the Department of Zoology of the Hungarian Natural History Museum. We are also grateful to Dr. Günther P. Können for reading and commenting on an earlier version of the manuscript. Many thanks also for the constructing comments of two anonymous reviewers.

Appendix A. Measurement of linear and circular polarization

The state of polarization of light at a given wavelength λ can be described by four independent parameters. In our work, we used the Stokes formalism, in which the state of polarization is described by the Stokes vector $\underline{S}$ possessing four components (S_0, S_1, S_2, and S_3). Component S_0 is the intensity; components S_1 and S_2 describe the linear polarization, while component S_3 characterizes the circular polarization. To any optical element a 4×4 Mueller matrix $\underline{\underline{M}}$ can be assigned, which matrix describes how the element changes the Stokes vector $\underline{S}$ of the incoming light (Collett, 1993):

$$\underline{S}' = \underline{\underline{M}}\cdot\underline{S}, \tag{1}$$

where $\underline{S}'$ is the Stokes vector of outcoming light after the interaction with the optical element. Since only the light intensity S_0' can be measured directly, four independent measurements of the intensity of outcoming light are required to determine the state of polarization $\underline{S}$ of the incoming light. In each of these four measurements we need the intensity of the same light transmitted through four different optical elements characterized by different Mueller matrices. These optical elements should change separately or simultaneously the linear and circular polarization of the incoming light. Thus, in a general case the determination of the Stokes parameters of the incoming light is the following: Let the Stokes vector of the incoming light (that is the light entering the polarimeter) be

$$\underline{S}_{\text{in}} = (S_0, S_1, S_2, S_3) \tag{2}$$

and let the Mueller matrices of the mentioned four different optical elements be $\underline{\underline{M}}^{(0)}$, $\underline{\underline{M}}^{(1)}$, $\underline{\underline{M}}^{(2)}$, and $\underline{\underline{M}}^{(3)}$. Construct the vector $\underline{I}(I_0, I_1, I_2, I_3)$, where

$$I_j = \sum_k M_{0k}^{(j)} S_k \tag{3}$$

is the measured intensity of light outcoming from the j-th optical element. Compose a 4×4 matrix $\underline{\underline{F}}$, the j-th and k-th ($0 \leqslant j, k \leqslant 3$) element of which is

$$F_{jk} = M_{0k}^{(j)}. \tag{4}$$

Matrix $\underline{\underline{F}}$ satisfies the equation

$$\underline{\underline{F}}\cdot\underline{S}_{\text{in}} = \underline{I}. \tag{5}$$

If the inverse matrix $\underline{\underline{F}}^{-1}$ of $\underline{\underline{F}}$ exists, the Stokes vector $\underline{S}_{\text{in}}$ of the incoming light can be obtained as follows:

$$\underline{S}_{\text{in}} = \underline{\underline{F}}^{-1}\cdot\underline{I}. \tag{6}$$

In our measurements we used four (three left-handed and one right-handed) neutral density (grey) circular polarizers made of the same material, and characterized by a practically constant absorption spectrum for wavelengths $400\text{ nm} < \lambda < 750\text{ nm}$, but with different orientations of the crystal axes of their $\lambda/4$ retarders. This method has the advantage that the absorption spectra of all four polarizers are the same. A left- and right-circular polarizer consists of a $\lambda/4$ retarder and a linear polarizer, the transmission axis of which is rotated by 45° clockwise and counter-clockwise relative to the crystal axis of the retarder, respectively. The incoming light is first transmitted through the linear polarizer, and then through the $\lambda/4$ retarder. The transmitted light becomes left- or right-circularly polarized (Fig. 7) and its intensity depends on the linear polarization of the incoming light. Thus a circular polarizer functions as a linear analyzer, when measuring the intensity of light transmitted through it.

If the circular polarizer is reversed (the light is first transmitted through the $\lambda/4$ retarder and then through the linear polarizer), then the transmitted light becomes linearly polarized, and its intensity depends on the circular polarization of the incoming light (Collett, 1993). It means that a reversed circular polarizer functions as a circular analyzer, when measuring the intensity of light transmitted through it.

The x and y components of the electric field vector ($\underline{E}$-vector) of light transmitted through a $\lambda/4$ retarder suffers

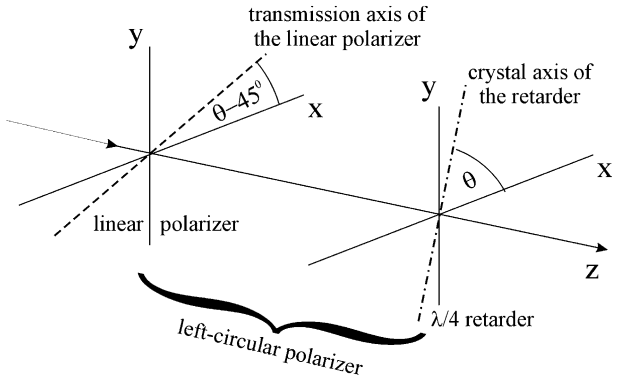

Fig. 7. A left-circular polarizer is composed of a $\lambda/4$ retarder (the crystal axis of which is aligned at angle θ relative to axis x) and a linear polarizer (the transmission axis of which is rotated by $-45°$ from the crystal axis of the retarder). The incoming light is first transmitted through the linear polarizer, and then through the $\lambda/4$ retarder. A circular polarizer is characterized by angle θ in this work.

a $\pi/4$ and $-\pi/4$ phase shift, respectively, thus the Mueller matrix of a $\lambda/4$ retarder is (Collett, 1993):

$$\underline{\underline{M}}_{\lambda/4} = \begin{pmatrix} 1 & 0 & 0 & 0 \\ 0 & 1 & 0 & 0 \\ 0 & 0 & 0 & -1 \\ 0 & 0 & 1 & 0 \end{pmatrix}. \tag{7}$$

The Mueller matrix of a linear polarizer, the transmission axis of which is parallel to the x axis is (Collett, 1993):

$$\underline{\underline{M}}_{\mathrm{LIN}} = \frac{1}{2}\begin{pmatrix} 1 & 1 & 0 & 0 \\ 1 & 1 & 0 & 0 \\ 0 & 0 & 0 & 0 \\ 0 & 0 & 0 & 0 \end{pmatrix}. \tag{8}$$

If the Mueller matrix of an optical element is $\underline{\underline{M}}$, its Mueller matrix after a rotation by angle θ around the z axis is (Collett, 1993):

$$\underline{\underline{M}}(\theta) = \underline{\underline{M}}_{\mathrm{ROT}}(-\theta) \cdot \underline{\underline{M}} \cdot \underline{\underline{M}}_{\mathrm{ROT}}(\theta), \tag{9}$$

where

$$\underline{\underline{M}}_{\mathrm{ROT}}(\theta) = \begin{pmatrix} 1 & 0 & 0 & 0 \\ 0 & \cos 2\theta & \sin 2\theta & 0 \\ 0 & -\sin 2\theta & \cos 2\theta & 0 \\ 0 & 0 & 0 & 1 \end{pmatrix} \tag{10}$$

is the Mueller matrix of the rotator (i.e. the operator that rotates an element by angle θ). θ is measured from axis x counter-clockwise (Fig. 7). In order to determine the state of polarization of light reflected from the target towards the polarimeter, let us apply three left-circular polarizers (linear analyzers) and one reversed right-circular polarizer (right-circular analyzer) in the four independent measurements. We used three left-circular filters (filters 1, 2, and 3 in Fig. 1) with light entering on the side where no quarter lambda plate was present, as a tool to determine the linear state of polarization. This was done to keep the optical properties of the four filters the same. Hence, the linear analyzers 1–3 were actually left-circular polarizers mounted normally in front of the camera (Fig. 1C). According to the above, the Mueller matrix of such a left-circular polarizer (LCP) (Fig. 7) is:

$$\begin{aligned} \underline{\underline{M}}_{\mathrm{LCP}}(\theta) &= \underline{\underline{M}}_{\lambda/4}(\theta) \cdot \underline{\underline{M}}_{\mathrm{LIN}}(\theta - 45°) \\ &= \frac{1}{2}\begin{pmatrix} 1 & \sin 2\theta & -\cos 2\theta & 0 \\ 0 & 0 & 0 & 0 \\ 0 & 0 & 0 & 0 \\ -1 & -\sin 2\theta & \cos 2\theta & 0 \end{pmatrix}. \end{aligned} \tag{11}$$

Similarly, the Mueller matrix of a reversed right-circular polarizer (revRCP) is:

$$\begin{aligned} \underline{\underline{M}}_{\mathrm{revRCP}}(\theta) &= \underline{\underline{M}}_{\mathrm{LIN}}(\theta - 45°) \cdot \underline{\underline{M}}_{\lambda/4}(\theta) \\ &= \frac{1}{2}\begin{pmatrix} 1 & 0 & 0 & 1 \\ \sin 2\theta & 0 & 0 & \sin 2\theta \\ -\cos 2\theta & 0 & 0 & -\cos 2\theta \\ 0 & 0 & 0 & 0 \end{pmatrix}. \end{aligned} \tag{12}$$

Thus, the Stokes vector of the light transmitted through a left-circular polarizer (LCP) is:

$$\begin{aligned} \underline{S}_{\mathrm{LCP}}(\theta) &= \underline{\underline{M}}_{\mathrm{LCP}}(\theta) \cdot \underline{S}_{\mathrm{in}} \\ &= \frac{S_0 + S_1 \sin 2\theta - S_2 \cos 2\theta}{2}\begin{pmatrix} 1 \\ 0 \\ 0 \\ -1 \end{pmatrix}. \end{aligned} \tag{13}$$

According to Eq. (13), the intensity of light transmitted through a reversed left-circular polarizer depends on the linear polarization of the incoming light. The Stokes vector of the light transmitted through a reversed right-circular polarizer (revRCP) is:

$$\underline{S}_{\mathrm{revRCP}}(\theta) = \underline{\underline{M}}_{\mathrm{revRCP}}(\theta) \cdot \underline{S}_{\mathrm{in}} = \frac{S_0 + S_3}{2}\begin{pmatrix} 1 \\ \sin 2\theta \\ -\cos 2\theta \\ 0 \end{pmatrix}. \tag{14}$$

Thus, the intensity of light transmitted through a reversed right-circular polarizer depends on the circular polarization (component S_3) of the incoming light (and same is true for a reversed left-circular polarizer, as well). It means that using a reversed circular polarizer, one can determine with the naked eye whether the incoming light is left- or right-circularly polarized or circularly unpolarized. For us only the intensity S_0 of the transmitted light is important, because this is the only measurable component. Thus, if the incoming light is transmitted through three left-circular polarizers (linear analyzers) characterized by angles θ_1, θ_2, and θ_3 (Fig. 7) and then through one reversed right-circular polarizer sequentially in four independent measurements, we obtain the following four intensities of the outcoming light:

$$
\begin{aligned}
I_{\mathrm{LCP}}(\theta_1) &= \frac{S_0 + S_1 \sin 2\theta_1 - S_2 \cos 2\theta_1}{2},\\
I_{\mathrm{LCP}}(\theta_2) &= \frac{S_0 + S_1 \sin 2\theta_2 - S_2 \cos 2\theta_2}{2},\\
I_{\mathrm{LCP}}(\theta_3) &= \frac{S_0 + S_1 \sin 2\theta_3 - S_2 \cos 2\theta_3}{2},\\
I_{\mathrm{revRCP}} &= \frac{S_0 + S_3}{2}.
\end{aligned}
\tag{15}
$$

It is obvious that the intensity of light transmitted through a reversed right-circular polarizer does not depend on the orientation of the transmission axis of its linear polarizer component, thus the orientation of the reversed circular polarizer is arbitrary. Eq. (15) constitute a system of equations with the four unknown variables S_0, S_1, S_2, and S_3, corresponding to the general matrix Eq. (5). Let us introduce the parameters

$$
A = \frac{\sin 2\theta_2}{\sin 2\theta_1}, \quad B = \frac{\sin 2\theta_3}{\sin 2\theta_1}, \tag{16}
$$

where $\theta_1 \neq n \cdot \pi$ ($n = 0, \pm 1, \pm 2, \ldots$). Solving the system of Eq. (15), we obtain the components of the Stokes vector of the incoming light:

$$
\begin{aligned}
S_2 &= 2\frac{I_{\mathrm{LCP}}(\theta_3)(1-A) - I_{\mathrm{LCP}}(\theta_2)(1-B) + I_{\mathrm{LCP}}(\theta_1)(A-B)}{(\cos 2\theta_2 - A\cos 2\theta_1)(1-B) + (B\cos 2\theta_1 - \cos 2\theta_3)(1-A)},\\
S_1 &= \frac{[2I_{\mathrm{LCP}}(\theta_1) + S_2 \cos 2\theta_1](1-A) - 2I_{\mathrm{LCP}}(\theta_2) + S_2(A\cos 2\theta_1 - \cos 2\theta_2) + 2AI_{LCP}(\theta_1)}{(1-A)\sin 2\theta_1},\\
S_0 &= \frac{2I_{\mathrm{LCP}}(\theta_2) - S_2(A\cos 2\theta_1 - \cos 2\theta_2) - 2AI_{\mathrm{LCP}}(\theta_1)}{1-A},\\
S_3 &= 2I_{\mathrm{revRCP}} - S_0.
\end{aligned}
\tag{17}
$$

By calculating these components of the incoming Stokes vector, the state of polarization of the incoming light is completely determined. In the investigation of the reflection–polarization patterns of scarab beetles we used the following more expressive variables:

$$
\text{degree of linear polarization} : p = \frac{\sqrt{S_1^2 + S_2^2}}{S_0} \tag{18}
$$

$$
\text{angle of polarization} : \alpha = \frac{1}{2}\arctan\left(\frac{S_2}{S_1}\right), \tag{19}
$$

$$
\text{ellipticity} : \varepsilon = \frac{1}{2}\arcsin\left(\frac{S_3}{S_0}\right). \tag{20}
$$

These variables also fully describe the state of (linear and circular) polarization. Ellipticity describes both the handedness (left: ε is negative; right: ε is positive) and the degree of circular polarization (which is usually defined as $p_{\mathrm{circ}} = S_3/S_0$). The ellipticity of completely left- and right-circularly polarized light is $-45°$ and $+45°$, respectively, while circularly unpolarized light has an ellipticity of 0°.

Considering the aim of our present study, ellipticity (or the degree of circular polarization) is the most important variable, therefore we also account for its measurement errors. These errors originate from the errors of the four intensity measurements. Apart from the artefacts (see Materials and Methods), they originate from two sources: (i) The inaccuracy of angles θ_1, θ_2, and θ_3 characterizing the three left-circular polarizers (linear analyzers) (Fig. 7). In our polarimeter this inaccuracy was $\pm 1°$. (ii) The "quantum noise" originating from the digitization of the intensity values recorded by the camera. Since error (ii) was much more significant, (i) was neglected. Let a polarization variable W depend on the measured intensities $I_{\mathrm{LCP}}(\theta_1)$, $I_{\mathrm{LCP}}(\theta_2)$, $I_{\mathrm{LCP}}(\theta_3)$ and I_{revRCP}. The absolute error of W originating from the quantum noise is:

$$
\Delta_q W = \left[\left|\frac{\partial W}{\partial I_{\mathrm{LCP}}(\theta_1)}\right| + \left|\frac{\partial W}{\partial I_{\mathrm{LCP}}(\theta_2)}\right| + \left|\frac{\partial W}{\partial I_{\mathrm{LCP}}(\theta_3)}\right| + \left|\frac{\partial W}{\partial I_{\mathrm{revRCP}}}\right|\right]\Delta q, \tag{21}
$$

where Δq is the quantum noise of the measured intensities. Δq is determined by the resolution of the A/D converter in the digital camera of the polarimeter and by the resolution of data file storing the digital intensity values. Thus, the absolute error of ellipticity originating from the quantum noise is:

$$
\Delta_{\mathrm{q}}\varepsilon = \left|\frac{\Delta_{\mathrm{q}} S_3}{2S_0\sqrt{1 - \frac{S_3^2}{S_0^2}}}\right| + \left|\frac{S_3 \cdot \Delta_{\mathrm{q}} S_0}{2S_0^2\sqrt{1 - \frac{S_3^2}{S_0^2}}}\right|, \tag{22}
$$

where the errors $\Delta_{\mathrm{q}} S_3$ and $\Delta_{\mathrm{q}} S_0$ are calculated according to expression Eq. (21). These values are constant due to the linear dependence of S_3 and S_0 on the measured intensities. Here, we omit to give the extensive expressions of $\Delta_{\mathrm{q}} S_3$ and $\Delta_{\mathrm{q}} S_0$.

References

Caveney, S. (1971). Cuticle reflectivity and optical activity in scarab beetles: The role of uric acid. *Proceedings of the Royal Society of London B, 178*, 205–225.

Collett, E. (1993). *Polarized light—fundamentals and applications*. New York, Basel, Hong Kong: Marcel Dekker.

Gokan, N., & Meyer-Rochow, V. B. (2000). Morphological comparisons of compound eyes in Scarabaeoidea (Coleoptera) related to the beetles' daily activity maxima and phylogenetic positions. *Journal of Agricultural Science (Tokyo), 45*, 16–61.

Horváth, G., & Varjú, D. (2003). *Polarized light in animal vision–polarization patterns in nature*. Heidelberg, Berlin, New York: Springer.

Kattawar, G. W. (1994). A search for circular polarization in nature. *Optics and Photonics News September*, 42–43.

Können, G. P. (1985). *Polarized light in nature*. Cambridge: Cambridge University Press.

Michelson, A. A. (1911). On metallic colouring in birds and insects. *Philosophical Magazine, 21*, 554–567.

Neville, A. C., & Caveney, S. (1969). Scarabaeid beetle exocuticle as an optical analogue of cholesteric liquid crystals. *Biological Review, 44*, 531–562.

Neville, A. C., & Luke, B. M. (1971). Form optical activity in crustacean cuticle. *Journal of Insect Physiology, 17*, 519–526.

Robinson, C. (1966). The cholesteric phase in polypeptide solutions and biological structures. *Molecular Crystals, 1*, 467–494.

Umow, N. (1905). Chromatische Depolarisation durch Lichtzerstreuung. *Physikalische Zeitschrift, 6*, 674–676.

Wynberg, H., Meijer, E. W., Hummelen, J. C., Dekkers, H. P. J. M., Schippers, P. H., & Carlson, A. D. (1980). Circular polarization observed in bioluminescence. *Nature, 286*, 641–642.